

Titanium Infiltration into ultra-thin PMMA Brushes

P. G. Mani-Gonzalez,^{2, b)} C. McFeely,¹ M. Snelgrove,¹ K. Shiel,¹ J.A. Hernandez Marquez,² R. O'Connor^{1,3}

¹ School of Physical Sciences, Dublin City University, Glasnevin, Dublin 9, Ireland

² Institute of Engineering and Technology, Department of Physics and Mathematics, Autonomous University of Ciudad Juárez, Cd. Juárez 32310, México

³ Advanced Processing Technology Centre, Dublin City University, Glasnevin, Dublin 9, Ireland

b) Electronic mail: pierre.mani@uaci.mx

Vapor phase infiltration (VPI) is a bottom up process that involves the infiltration of polymers, often using atomic layer deposition (ALD) compatible precursors. By exposing a polymer to an organo-metallic precursor, area selective material formation is achieved where the precursor reacts with regions covered by an infiltration-receptive polymer brush. Combining receptive and rejecting polymers which have the capability to form complex nanopatterns could potentially allow for the creation of nanofeatures, offering a route to area selective deposition (ASD). This work is concerned with the creation and characterisation of titanium infiltrated films with a VPI process. Thin films of poly (methyl methacrylate) (PMMA) were infused with titanium isopropoxide (TTIP) and subsequently analysed with angular resolved X-ray photoelectron spectroscopy (ARXPS). All XPS analysis and VPI treatments were completed without breaking vacuum in an integrated ultra-high vacuum setup, with O 1s, C 1s, Ti 2p and Si 2p core levels revealing the successful incorporation of titanium into the polymer. Grazing angle Fourier-transform infrared spectroscopy (GA-FTIR) demonstrates the breaking of carbon-oxygen double bonds within the PMMA structure due to titanium incorporation.

I. INTRODUCTION

The use of atomic layer deposition (ALD) as a technique to obtain thin films of inorganic materials through gas phase precursors is a widely studied area.¹ For area selective deposition (ASD), techniques involving the use of ALD – like processes are considered as an alternative to traditional top-down patterning such as optical lithography. This includes polymer infiltration through vapor phase infiltration (VPI), which can be subcategorized into several processes, which includes sequential infiltration synthesis (SIS).^{2,3,4} A SIS process implements typical ALD parameters but with extended sample exposure to precursors.^{5, 6} Whereas ALD is concerned with the deposition of a material (via a precursor) onto a surface, SIS relies upon the infiltration of the precursor into a receptive, reactive polymer film. The use of polymers to address ASD and optical lithography issues are in part due to the capability of polymers to form Block Copolymers (BCP). A BCP is a material compound of two or more combined polymers with different polar properties capable of self-arranging into various morphologies based on their individual characteristics.^{7, 8} Some of the polymers suitable for BCP lithography include Polystyrene (PS), Poly(2-vinylpyridine) (P2VP) and Poly(methyl methacrylate) (PMMA), Poly(ethylene oxide) (PEO), Poly(Lactic Acid) (PLA) and SU-8.^{9,10,11,12,13,14,15} PMMA possesses both good thermal stability withstanding temperatures from 150 °C to 200 °C as well as being considered a receptive polymer suitable for VPI infiltration. Previous SIS studies on PMMA have been predominately focused on its strong chemical reaction with Trimethylaluminum (TMA), resulting in aluminum infiltration throughout the polymer.¹⁶ This reaction occurs through the breaking of the oxygen double bond within PMMA. Understanding how other ALD precursors interact with PMMA is of interest so as to understand the polymer's

suitability for a broad range of microelectronics applications.¹⁷ This work focuses on titanium infiltration into thin films of PMMA brushes using titanium isopropoxide (TTIP) as the precursor. TTIP has previously been reported to have limited infiltration into thick films of PMMA due to the sizing of the precursor.¹⁸ In order to study how the process scales to films of a compatible thickness for semiconductor industry applications, this letter employs angle resolved X-ray photoelectron spectroscopy (ARXPS) to analyse in detail the degree of TTIP interaction with, and infiltration into PMMA.¹⁹

II. EXPERIMENTAL

Hydroxy-terminated PMMA (molecular weight: 40 kg/mol) was purchased from Polymer Source and dissolved in toluene (wt. %: 1.0). The solution was spin coated onto OH-terminated Si (prepared via oxygen plasma) and annealed at 230°C for 24 hours. Ellipsometer measurements revealed the presence of an approximately 8 nm film atop of the Si.

The SIS processing took place in a custom-built vacuum chamber (base pressure: 1×10^{-3} mbar) coupled in-vacuum to an XPS system (base pressure: 5×10^{-10} mbar) equipped with an Al K α ($h\nu = 1486.7$ eV) X-ray source. This setup allowing for sample transfer from the ALD to XPS chamber without breaking vacuum. The PMMA films were heated at 190 - 195°C for 20 minutes prior to the SIS process beginning.^{20, 21} This temperature was within the “ALD window” for TTIP titanium deposition inhibition. A SIS cycle consisted of the following; **(a)** A 10 s N₂ purge. **(b)** Pumping to all the pressure to recover to approximately 5×10^{-2} mbar before the chamber was isolated from pumping and a 2.5 s TTIP dose was performed **(c)** A 300 s ‘hold time’ – where the chamber was left under static vacuum (no pumping). At the end of this step, normal pumping was resumed. This cycle was repeated

five times (as Figure 1 shows). Adding a water dose step to the process was not desired, as the addition of co-reactants can allow non-reactive polymers to incorporate precursors,²² use external agent as water reduce the ASD capabilities as was supported in our previous work.²³ Grazing angle Fourier transform infrared spectroscopy (GA-FTIR) was performed ex-situ in order to look at the chemical interaction between the PMMA and the TTIP precursor. GA-FTIR was undertaken using a Nicolet IS50 FTIR Spectrometer with a Harrick VariGATR attachment. Each sample was scanned at an un-polarized angle of incidence of 65° for a total of 128 scans and at 8cm^{-1} resolution.

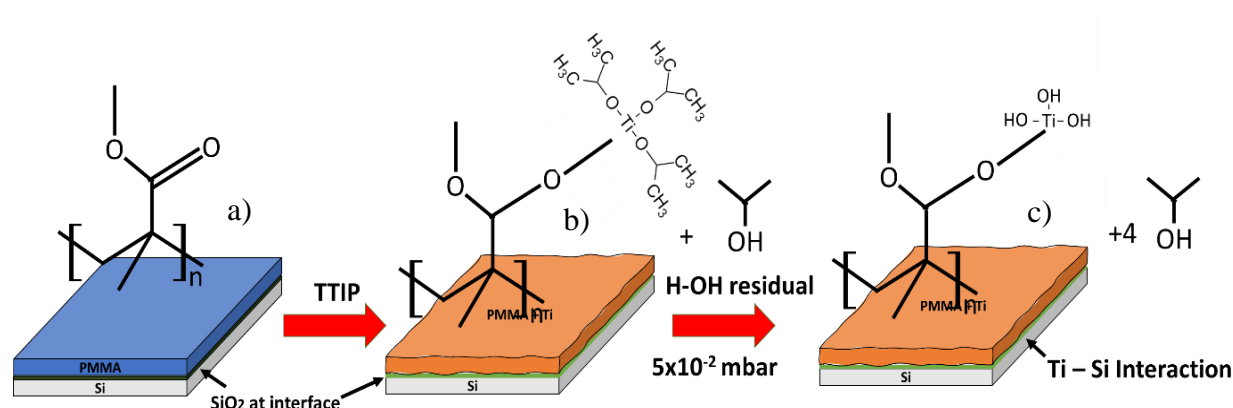


Figure 1. Reaction schematic between TTIP and PMMA, a) N₂ purge, b) pumping to 5×10^{-2} mbar and c) 300 s waiting after TTIP dose.

III. RESULTS AND DISCUSSION

The C 1s signal before and after TTIP infiltration is shown in Figure 2. C-C, C-O and C=O were located at 285.47 eV, 287.2 eV and 289.3 eV respectively. All signals were associated with that of PMMA. Crucially, after TTIP exposure, the C=O component of the C 1s is diminished, suggesting TTIP interaction, similar to what is observed in PMMA – TMA processes (as reference 16 describes). Minimum change is observed in the C-C and C-O

component, highlighting that the precursor reaction is limited to the carbonyl group of the PMMA only.

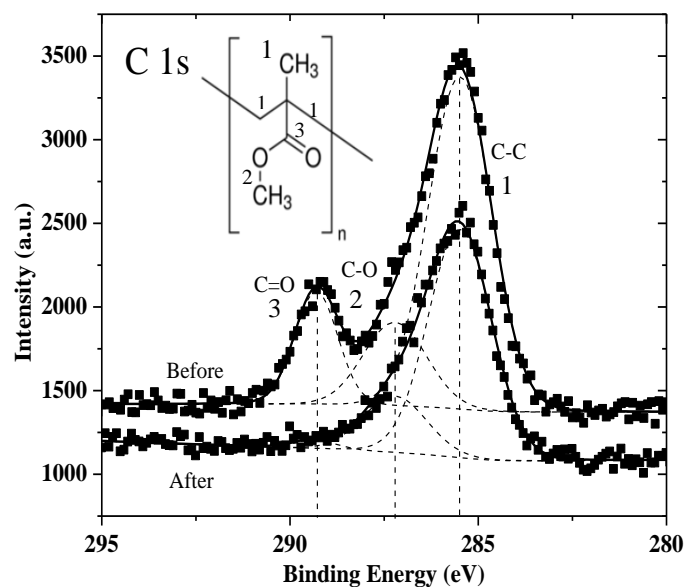


Figure 2. C 1s (90° take-off angle normal emission) before and after TTIP infiltration on PMMA. Post TTIP exposure, the C=O signal is diminished due to TTIP – PMMA interaction.

The Ti $2p$ peak was fitted with four signals as shows in Figure 3a). The deconvolution process for the Ti $2p$ signal had to account for the Coster-Kronig effect, and it is important to note that the analysis employed used a doublet splitting of 5.7 eV and a spin-orbit coupled state ratio of 0.43.^{24,25} This is to account for the fast Auger emission effect occurring in the Ti $2p_{1/2}$. Broadening of the Ti $2p_{1/2}$ component also occurs, requiring that the Gaussian value of the fit was increased from 1.2 eV (Ti $2p_{3/2}$) to 1.46 eV (Ti $2p_{1/2}$), whereas the Lorentzian value was decreased from 1.2 to 0.66 respectively. The $3/2$ component positions are as follows, Ti⁺² was associated to TiO at 454.2 eV (± 0.1 eV) and attributed at the atmosphere – sample interface. Ti⁺³ was associated to Ti₂O₃ at 457.2 eV (± 0.1 eV).²⁶ Ti⁺⁴ was associated

with the maximum signal at 459.85 eV as TiO_2 .²⁷ However, this signal also represents the more complex form of C-O-Ti-O as seen in Figure 2. Additionally, titanium silicates could also be attributed to some contribution of the titanium signals.

The O 1s core level was fitted with three signals as shown in Figure 3b. PMMA active sites containing oxygen form bonds with titanium, with Ti-O-PMMA or Ti-O-Ti bonds observed at 531.2 eV. Oxygen bonding with silicon was detected at 533.1 eV, with this signal arising from the native silicon oxide. The signal at 534.25 eV represents environment exposition as absorption water, some bonds with -OH at surface and C-O bonds in the PMMA structure.

The Si 2p peak shown in Figure 3c was used as a binding energy reference for all other peaks.

The Si^{+4} signal at 103.9 eV associating to silicon oxide increases with grazing angle. The signal at 101.9 eV, associated to Si^{+3} , suggests possible titanium silicon interaction, thus forming an unstable layer of $\text{Si}_x\text{Ti}_{1-x}\text{O}_y$ at the PMMA/ SiO_2 interface.

This is the author's peer reviewed, accepted manuscript. However, the online version of record will be different from this version once it has been copyedited and typeset.
PLEASE CITE THIS ARTICLE AS DOI: 10.1116/1.50001061

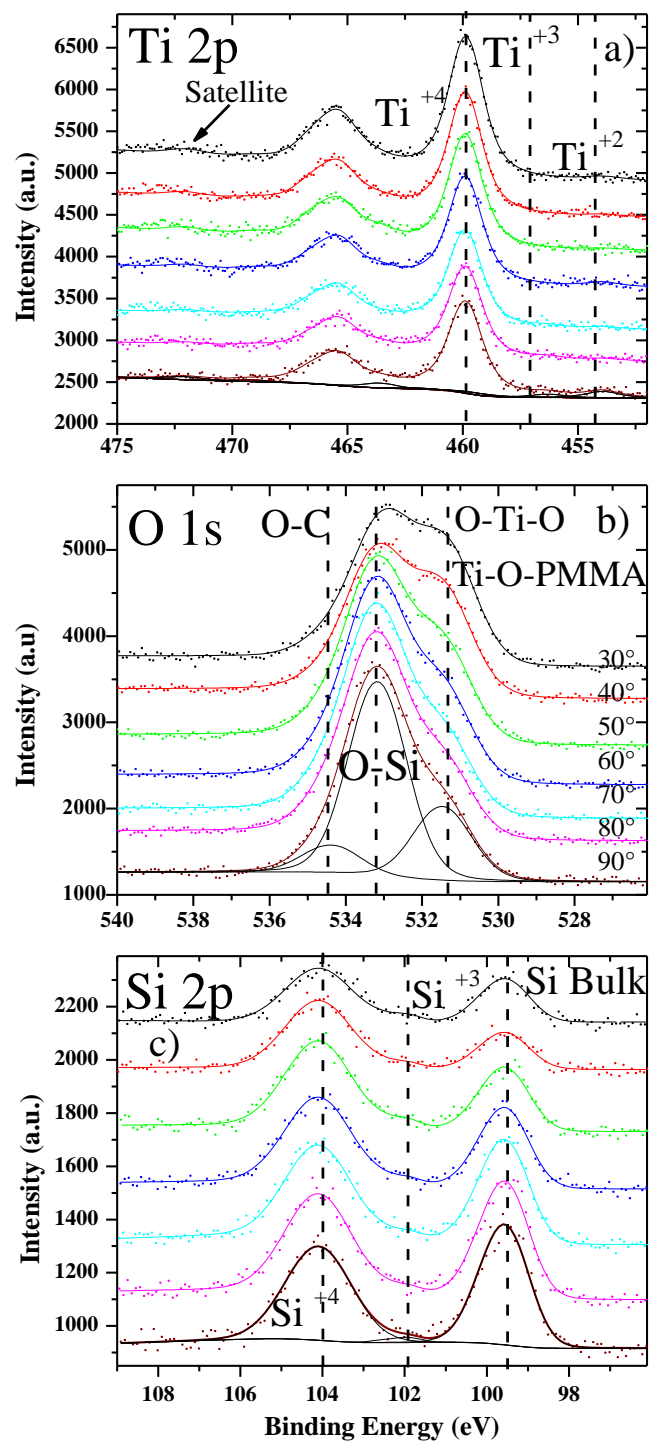


Figure 3. ARXPS of a) Ti 2p b) O 1s and c) Si 2p (Si Bulk at 99.4 eV used to shift all spectra) core levels of sample with TTIP infiltrated on PMMA/Si.

This is the author's peer reviewed, accepted manuscript. However, the online version of record will be different from this version once it has been copyedited and typeset.
PLEASE CITE THIS ARTICLE AS DOI: 10.1116/6.0001061

Figure 4 shows the FTIR spectra of PMMA pre and post TTIP infiltration. Peaks at 2929, 1450 and 900 cm^{-1} , which can be seen in both spectra, are associated with various bending and stretching modes of C-H bonds found mainly in the polymer backbone.²⁸ The band appearing at 1735 cm^{-1} in Figure 4a shows the presence of the C=O stretching vibration which is of great importance as it is this bond which facilitates the TTIP infiltration. After infiltration this band at 1735 cm^{-1} appears to be greatly reduced indicating the breaking of the C=O bonds, this can be seen in Figure 4b. The disappearance of this band indicates that there is a chemical interaction between the PMMA and the TTIP precursor.²⁹

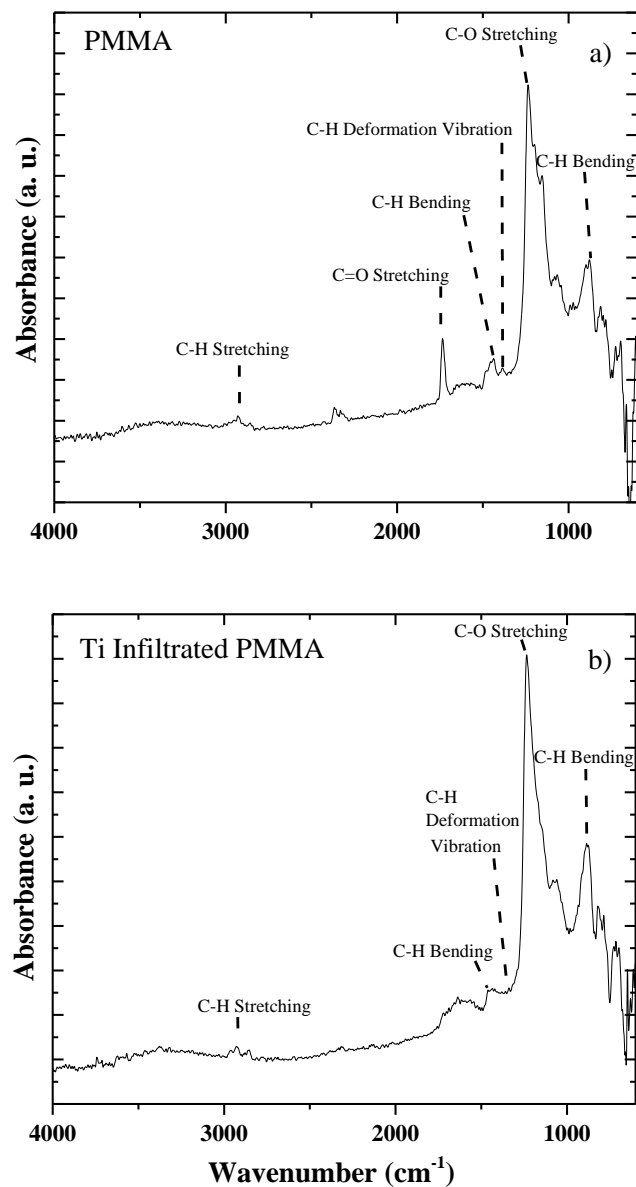


Figure 4. FTIR a) PMMA and b) Titanium infiltrated PMMA (this shows carbon bonds before a) and after b) Ti infiltration). Spectra have been corrected for baseline shift.

IV. SUMMARY AND CONCLUSIONS

TTIP was exposed to PMMA brushes with XPS and FTIR showing promising intake of titanium into the polymer film, driven by a strong reaction of the TTIP with the carbonyl

group of PMMA. Titanium signals according to ARXPS were distributed throughout the polymer film. The titanium incorporated in the PMMA film is in a multi oxidized state, with TiO₂, Ti₂O₃ and TiO species forming during this infiltration process. Silicon-titanium interaction was suggested due to suboxide presence observed in the Si 2*p* spectra. This study shows that PMMA brushes can be easily infiltrated with TTIP for the generation of titanium dioxide.

AUTHOR'S CONTRIBUTIONS

P.G. Mani-Gonzalez: Conceptualization, Methodology, Formal analysis, Investigation, Writing- original draft, Visualization, Validation. **C. McFeely:** Formal analysis, Investigation, Writing-review & editing. **M. Snelgrove:** Conceptualization, Methodology, Formal analysis, Investigation, Writing-review & editing. **K. Shiel:** Investigation, writing-review & editing. **J.A. Hernandez-Marquez:** Investigation, Writing-review & editing. **R. O'Connor:** Conceptualization, Resources, Writing- review & editing, Project administration, Funding acquisition.

ACKNOWLEDGEMENT

The Author's would like to acknowledge the technical support of Pat Wogan for the XPS-ALD equipment. This work has been facilitated with the financial support of Science Foundation Ireland (SFI) under Grant No. 12/RC/2278 and 16/SP/3809.

DATA AVAILABILITY

The data that support the findings of this study are available from the corresponding author upon reasonable request.

REFERENCES

- ¹ C. Cummins, R. Lundy, J. J. Walsh, V. Ponsinet, G. Fleury, M. A. Morris, *Nano Today* **35**, 100936 (2020).
- ² K. J. Park, J. M. Doub, T. Gougousi, and G. N. Parsons, *Appl. Phys. Lett.* **86**, 051903 (2005).
- ³ T. Mårtensson, P. Carlberg, M. Borgström, L. Montelius, W. Seifert, L. Samuelson, *Nano Letters* **4**, 699 (2004).
- ⁴ Q. Peng, Y. C. Tseng, S. B. Darling, J. W. Elam, *ACS Nano* **5**, 4600 (2011).
- ⁵ Q. Peng, Y. C. Tseng, S. B. Darling, J. W. Elam, *Adv. Mater.* **22**, 5129 (2010).
- ⁶ R. Z. Waldman, D. J. Mandia, A. Yanguas-Gil, A. B. F. Martinson, J. W. Elam, S. B. Darling, *J. Chem. Phys.* **151**, 190901 (2019).
- ⁷ C. Cummins, Michael A. Morris. *Microelectron. Eng.* **195**, 1 (2018).
- ⁸ C. J. Hawker, T. P. Russell. *MRS Bull.* **30**, 952 (2005).
- ⁹ C. Cummins, M. T. Shaw, M. A. Morris, *Macromol. rapid comm.* **38**, 1700252 (2017).
- ¹⁰ Morris, M. A. *Microelectron. Eng.* **132**, 207 (2015).
- ¹¹ R. Lundy, P. Yadav, A. Selkirk, E. Mullen, T. Ghoshal, C. Cummins, M. A. Morris, *Chem. Mater.* **31**, 9338 (2019).
- ¹² E. C. Dandley, C. D. Needham, P. S. Williams, A. H. Brozena, C. J. Oldham, G. N. Parsons, *J. Mater. Chem. C.* **2**, 9416 (2014).
- ¹³ B. Gong, D. H. Kim, G. N. Parsons, *Langmuir* **28**, 11906 (2012).
- ¹⁴ B. Gong and G. N. Parsons, *J. Mater. Chem.* **22**, 15672 (2012).
- ¹⁵ C. Y. Nam, A. Stein, K. Kisslinger, *J. Vac. Sci. Technol. B.* **33**, 06F201 (2015).
- ¹⁶ M. Biswas, J. A. Libera, S. B. Darling, J. W. Elam, *Chem Mater.* **26**, 6135 (2014).
- ¹⁷ C. Cummins, M. A. Morris, *Microelectron. Eng.* **195**, 74 (2018).
- ¹⁸ A. Sinha, D. W. Hess, C. L. Henderson, *J. Vac. Sci. Technol. B.* **25**, 1721 (2007).
- ¹⁹ Y. C. Tseng, Q. Peng, L. E. Ocola, J. W. Elam, S. B. Darling, *J. Phys. Chem. C.* **115**, 17725 (2011).
- ²⁰ W. Jang H. Jeon, H. Song, Ho. Kim, Hy. Kim, Hy. Jeon., *Phys. Status Solidi A* **212**, 2785 (2015).
- ²¹ G. J. Yuan, J. F. Xie, H. H. Li, H. L. Lu, Y. Z. Tian, *Coatings.* **9**, 806 (2019).
- ²² C. Z. Leng, M. D. Losego, *Mater. Horizons.* **4**, 747 (2017).
- ²³ M. Snelgrove, C. McFeely, , K. Shiel, G. Hughes, P. Yadav, C. Weiland, J. C. Woicik, P.G. Mani-Gonzalez, R. Lundy, M. A. Morris, E. McGlynn, R. O'Connor, *Mater. Adv.* **2**, 769 (2021).



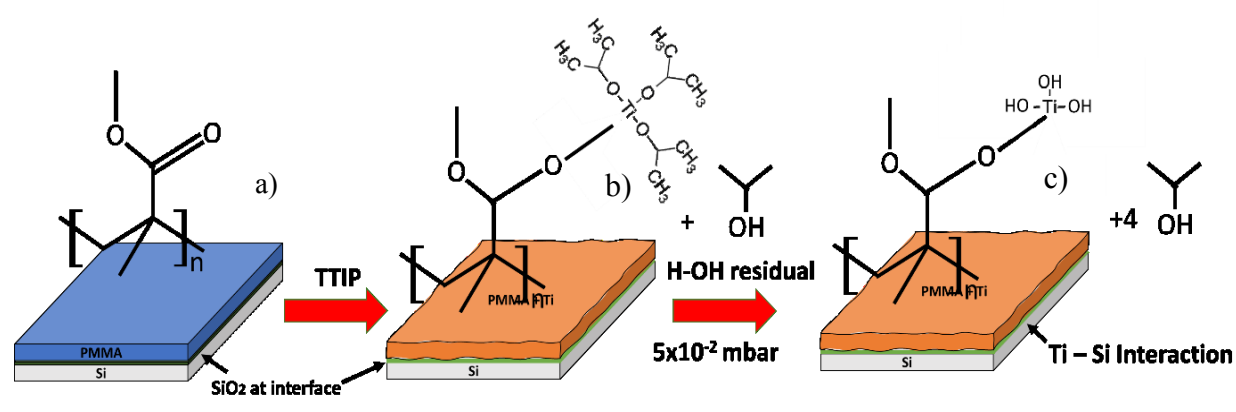
This is the author's peer reviewed, accepted manuscript. However, the online version of record will be different from this version once it has been copyedited and typeset.

PLEASE CITE THIS ARTICLE AS DOI: 10.1116/6.0001061

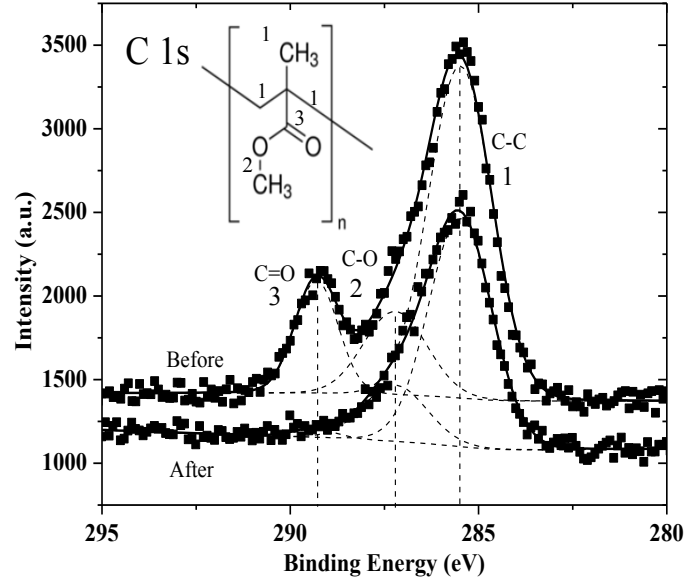
-
- ²⁴ M. Hannula, H. Ali-Löyty, K. Lahtonen, E. Sarlin, J. Saari, M. Valden, *Chem. Mater.* **30**, 1199 (2018).
- ²⁵ P. S. Bagus, C. Nelin, J. Brundle, R. Christopher, S. A. Chamber, *J. Phys. Chem. C.* **123**, 7705 (2018).
- ²⁶ Y. Hasegawa, A. Ayame, *Catal. Today* **71**, 177 (2001).
- ²⁷ R.M. Wang, C.L. Chu, T. Hu, Y.S. Dong, C. Guo, X.B. Sheng, P.H. Lin, C.Y. Chung, P.K. Chu, *Appl. Surf. Sci.* **253**, 8507 (2007).
- ²⁸ A. Alrahlah, H. Fouad, M. Hashem, A. A. Niazy, A. AlBadah, *Materials* **11**, 1096 (2018).
- ²⁹ D. C. Lee, L. W. Jang, *J. Appl. Polym. Sci.* **61**, 1117 (1996).

This is the author's peer reviewed, accepted manuscript. However, the online version of record will be different from this version once it has been copyedited and typeset.

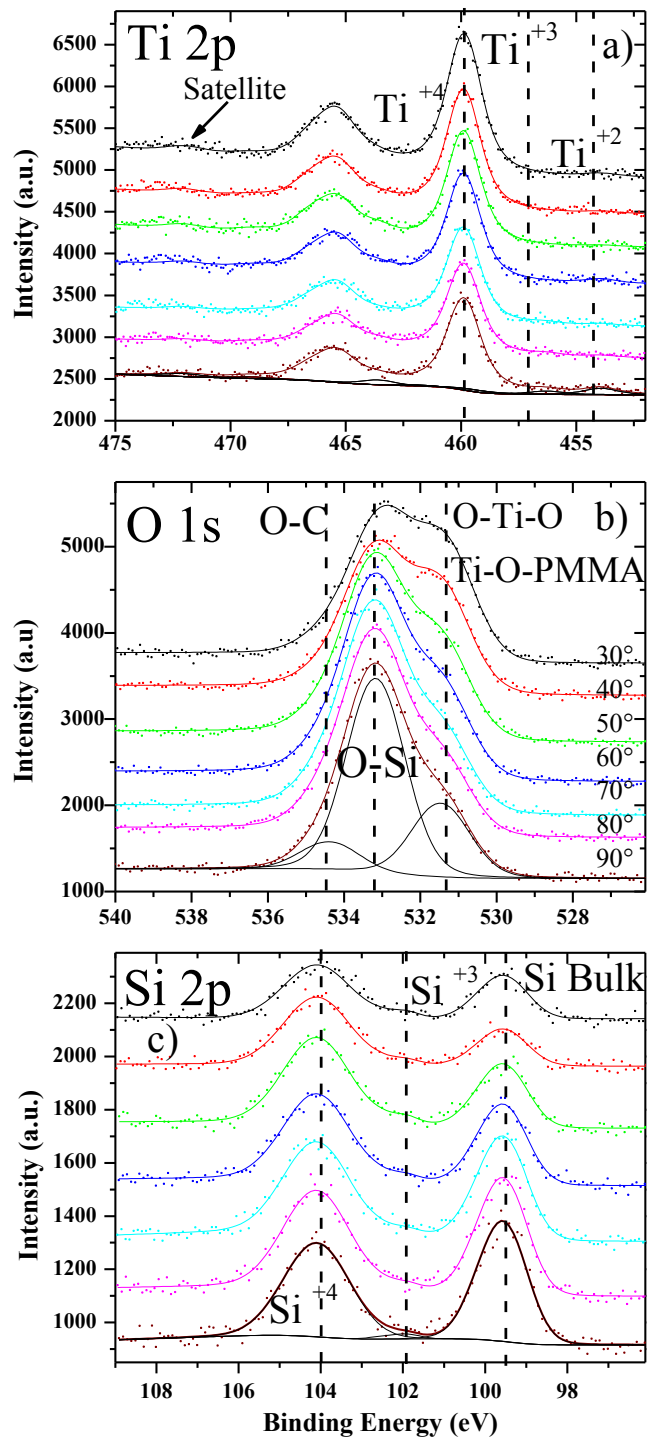
PLEASE CITE THIS ARTICLE AS DOI: 10.1116/6.0001061



This is the author's peer reviewed, accepted manuscript. However, the online version of record will be different from this version once it has been copyedited and typeset.
PLEASE CITE THIS ARTICLE AS DOI: 10.1116/6.0001061



This is the author's peer reviewed, accepted manuscript. However, the online version of record will be different from this version once it has been copyedited and typeset.
PLEASE CITE THIS ARTICLE AS DOI: 10.1116/1.6.0001061



This is the author's peer reviewed, accepted manuscript. However, the online version of record will be different from this version once it has been copyedited and typeset.
PLEASE CITE THIS ARTICLE AS DOI: 10.1116/6.0001061

